ORIGINAL ARTICLE

lajss.org
Latin American Journal of Solids and Structures

www.lajss.org

Investigation of Quasi-Static and Dynamic Mechanical Properties of Bio-Inspired Thin-Walled Structures under Axial Crushing

Zhanhong Guo[a,b], Na Han[a*], Meng Zou[a*], Yansong Liu[a], Jing Liu[c]

[a]Key Laboratory for Bionics Engineering of Education Ministry, Jilin University, Changchun 130022, China. E-mails: zhguojlu@163.com, hanna21_jlu@163.com, zoumeng@jlu.edu.cn, liuys23@mails.jlu.edu.cn

[b]College of Mechanical and Electronic Engineering, Tarim University, Alar 843300, China.

[c]College of Fashion and Textiles, Tarim University, Alar 843300, China. E-mails: 17767526319@163.com

* Corresponding author

https://doi.org/10.1590/1679-7825/e8621

Abstract

This study proposes a bio-inspired thin-walled energy-absorbing structure with self-similar configurations mimicking conch shells. Through quasi-static compression and drop hammer impact tests, the energy absorption characteristics were comparatively analyzed between the bio-inspired and conventional thin-walled tubes. The results demonstrate that under quasi-static compression, the bio-inspired tubes exhibit stable progressive buckling deformation, with a 21.39% increase in mean crush force (MCF) and a 12.95% improvement in crush force efficiency (CFE). During dynamic impact conditions, the bio-inspired structures show significantly reduced peak load while achieving enhanced specific energy absorption (SEA) and mean crush force (MCF), along with a 24.61% increase in crush force efficiency (CFE) and reduced undulation of load-carrying capacity (ULC). These findings offer novel perspectives for the development of innovative passive safety devices.

Keywords

thin-walled structures, bionic design, energy absorption, deformation mechanism, crashworthiness

Graphical Abstract

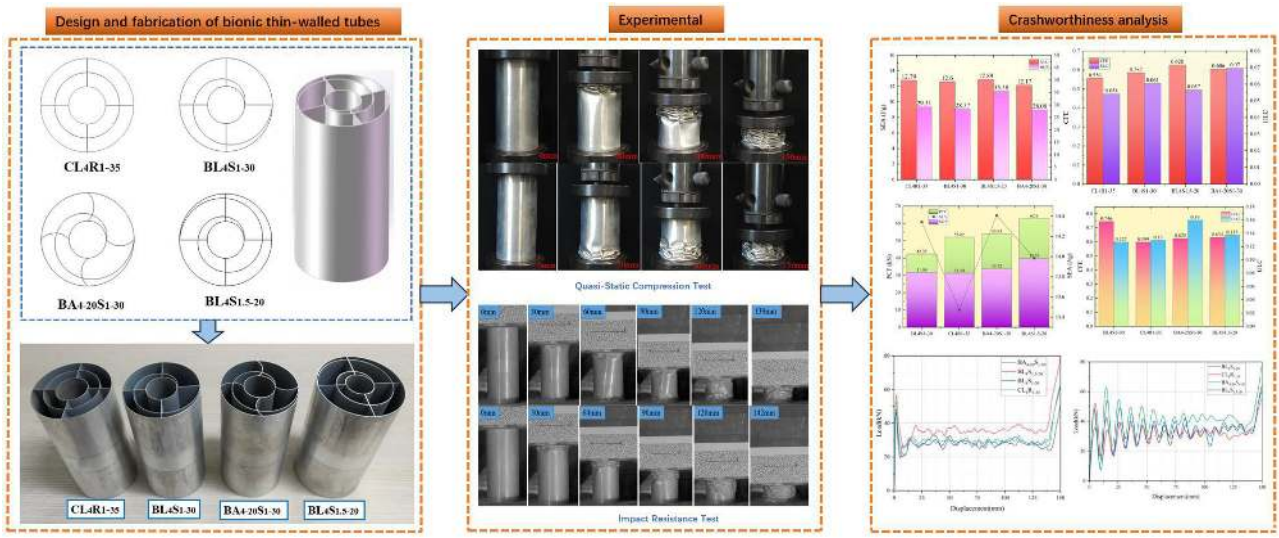

Received March 16, 2025. In revised form April 21, 2025. Accepted May 10, 2025. Available online May 13, 2025.
https://doi.org/10.1590/1679-7825/e8621

Latin American Journal of Solids and Structures. ISSN 1679-7825. Copyright © 2025. This is an Open Access article distributed under the terms of the Creative Commons Attribution license, which permits unrestricted use, distribution, and reproduction in any medium, provided the original work is properly cited.

1 INTRODUCTION

Thin-walled protective structures are widely adopted in automotive and rail transportation sectors due to their excellent mass-specific energy absorption capacity [Wu et al.,2021]. With the accelerating development trends of intelligent and green transportation equipment, there is an increasing demand for enhanced safety and lightweight design requirements of critical components in automobiles and rail systems [Li et al.,2024; Zhang et al.,2018a. However, indiscriminate mass reduction without systematic structural optimization may severely degrade crashworthiness. Therefore, studying the design of novel thin-walled structures and their impact response characteristics to maximize energy absorption *is crucial* for improving the passive safety performance of transportation equipment.

The research and development of thin-walled structures has continues to receive significant attention in the field of engineering materials, with researchers focusing on optimizing crashworthiness while achieving lightweight designs. Studies show that the crashworthiness of thin-walled tubes is influenced by multiple factors, including material mechanical properties, cross-sectional geometric characteristics, wall thickness dimensions, and loading conditions [Tang et al.,2013; Chen et al.,2023; Wang et al.,2023]. To replace traditional steel thin-walled tubes, researchers have successfully developed and applied a series of advanced lightweight materials, such as aluminum alloys, magnesium alloys, fiber-reinforced polymers (FRPs), and various hybrid material systems [Sun et al.,2022]. Albak E I. [2021] systematically investigated the crashworthiness of multi-cell circular corrugated thin-walled tubes under various loading conditions. Through integrated theoretical analysis and finite element simulations, they demonstrated that increasing the number of cells and optimizing the internal corner sections significantly improved the structure's impact resistance. Tran and Baroutaji [2018] innovatively proposed a multi-cell triangular tube design, achieved through internal rib connections to construct tubes with varying cell numbers. By integrating numerical simulations with predictive model development, they successfully established an accurate response surface model for the multi-cell triangular tubes. Furthermore, the Abdullahi research team [Abdullahi and Gao, 2020] developed a novel multi-cell structure based on Voronoi polygons, leveraging the stochastic characteristics of Voronoi diagrams to achieve randomized cell size distribution. Through finite element analysis and crash experiments, they demonstrated that compared to traditional uniform porous tubes, this design exhibited lower peak loads and superior energy absorption efficiency under axial compression. Wang et al. [2025] addressed the limitations of traditional honeycomb structures by developing a novel circular-reinforced re-entrant arc honeycomb (CRRAH) structure, inspired by the arch-shaped cell walls found in nature. By employing 3D printing technology and conducting quasi-static compression tests, they systematically investigated the mechanical properties and deformation patterns of the CRRAH structure with varying parameters.

Through natural selection and evolutionary processes, organisms have evolved structural characteristics with outstanding mechanical properties. These biological structures provide significant bio-inspired design inspiration for modern engineering, particularly which demonstrate value in optimizing the crashworthiness of thin-walled structures [Zhou et al.,2022]. Researchers have made substantial progress in enhancing structural performance by extracting structural features from biological prototypes and integrating them into thin-walled structure designs. In specific research efforts, Jiang et al. [2019] conducted experimental and finite element analyses to investigate the influence mechanisms of basic configuration elements (BCEs) on the crashworthiness of bio-inspired thin-walled structures, based on microstructural characteristics of beetle forewings and wild plants. Song et al. [2021] focused on the distinctive gradient structure features of bamboo, including its non-uniformly distributed fiber tissues and strength gradients varying with radial position, developing thin-walled tubes with gradient wall thickness. Regarding hierarchical bio-inspired structures, San Ha et al.[2021] innovatively integrated the cellular gradient distribution features of bones and bamboo to develop a novel bio-inspired hierarchical multi-cell square tube (BHMS). Analysis of its dynamic failure modes and energy absorption characteristics under axial compression revealed that the specific energy absorption of third-level BHMS tubes increased by 178.4% compared to first-level BHMS tubes, 173.7% relative to conventional square tubes, and 128.1% compared to multi-cell square tubes, demonstrating significant performance advantages. Additionally, Yin et al. [2015] designed a new bio-inspired thin-walled structure (BTS) based on horsetail plant characteristics. Finite element analysis of its crashworthiness under transverse impact loading showed superior performance compared to traditional circular and square tubes, with optimal configuration parameters varying with impact force thresholds. Zhang et al. [2018b] developed a novel multi-cell tube structure mimicking the microstructure of beetle forewings, with both experimental and numerical results confirming enhanced crashworthiness compared to conventional single-cell and multi-cell tubes. Song et al. [2024] investigated the static and dynamic mechanical properties of reed straw, proposing new approaches for designing lightweight, high-strength materials. Gao et al. [2023] introduced a bio-inspired hierarchical multi-cell hexagonal tube (BHMH) configuration based on biological gradient structures and hierarchical features. Their study demonstrated significantly enhanced crashworthiness in BHMH structures compared to traditional single-cell and multi-cell hexagonal tubes, with substantial improvements in maximum specific energy absorption values.

Conch shells have developed quantifiable protective properties in marine ecosystems, where they are frequently subjected to rock impacts and predator attacks. These biological structures effectively resist mechanical damage, exhibiting characteristics analogous to natural body armor [Ballarini and Heuer,2007]. The shell wall thickness is relatively small compared to the overall size of the conch, demonstrating a thin-walled structural configuration. Despite this, it can withstand loads significantly exceeding its own weight, highlighting its superior mechanical properties. Inspired by these structural characteristics, this study utilizes the conch shell as a biomimetic prototype to extract key structural elements for the design of lightweight yet high-strength thin-walled structures. To evaluate energy absorption performance, comparative experiments were conducted between conventional thin-walled tubes (CWT) and bionic conch tubes (BCT)structures fabricated via wire electrical discharge machining. Comprehensive testing protocols including quasi-static compression and dynamic drop hammer impact assessments were implemented, providing fundamental insights into crashworthiness enhancement strategies. These findings advance the development of innovative passive safety systems through biologically informed engineering solutions.

2 MATERIALS AND METHODS

2.1 Crashworthiness parameters

To comprehensively evaluate the crashworthiness of the biomimetic thin-walled tubes, four assessment metrics were selected: Specific Energy Absorption (SEA), Mean Crush Force (MCF), Crush Force Efficiency (CFE), and undulation of load-carrying capacity (ULC) [Liu et al.,2024].

The Specific Energy Absorption (SEA) represents the energy absorbed per unit mass of the energy-absorbing structure, defined as the ratio of the total energy absorption (EA) to the mass (M) of the energy-absorbing structure. A higher SEA value indicates better energy absorption performance. The expression is as follows:

$$SEA = \frac{EA}{M} \tag{1}$$

The Mean Crush Force (MCF) represents the impact load per unit compression distance, defined as the ratio of the total energy absorption (EA) to the maximum effective displacement. A higher MCF value indicates better energy absorption performance. The equation is as follows:

$$MCF = \frac{EA}{\delta_{\max}} \tag{2}$$

Peak Crush Force (PCF) represents the maximum crushing force during the entire compressive deformation process. Typically, the peak force observed is the initial peak crush force (IPCF), which occurs at the initial stage of compression. However, for certain fractal or filled structures, the peak force does not appear initially and instead corresponds to the global peak crush force (GPCF). In this experiment, PCF is defined as the GPCF, as follows:

$$PCF = F_{\max} \tag{3}$$

The Crush Force Efficiency (CFE) represents the stability of the impact load during the effective deformation process, serving as an indicator of the fluctuation in the impact load. The closer the CFE value is to 1, the higher the energy absorption efficiency. The equation is as follows:

$$CFE = \frac{MCF}{PCF} \tag{4}$$

The undulation of load-carrying capacity (ULC) is a dimensionless indicator that reflects the degree of fluctuation in the instantaneous impact load around the mean crush force during the compression process [Wen.M et al., 2020]. The smaller the ULC value, the smoother the load-displacement curve and the closer the load approaches a constant value, indicating a more efficient energy absorption process. The equation is as follows:

$$ULC = \frac{\int_0^{\delta_{max}} |F(x) - MCF| dx}{\int_0^{\delta_{max}} F(x) dx} \tag{5}$$

2.2 Geometric configuration

2.2.1 Structural and mechanical characteristics of conch shell

The morphological characteristics of conch shells are intrinsically linked to their growth processes. Through gradual secretion of biomineralized materials at the apertural margin of the protoconch, gastropods establish differential deposition rates between opposing sides, thereby generating spiral architectures. This growth mechanism maintains proportional scaling between newly formed and existing shell structures, exhibiting remarkable self-similar properties. Its shell is capable of withstanding impact loads from various directions, demonstrating exceptional mechanical properties. As shown in Figure 1(a), the shell material combines high hardness, lightweight characteristics, and superior corrosion resistance, enabling it to effectively endure multi-directional loads and impacts. During mechanical deformation, this structure exhibits remarkable energy absorption capabilities while maintaining high stiffness [Ghazlan et al.,2020].

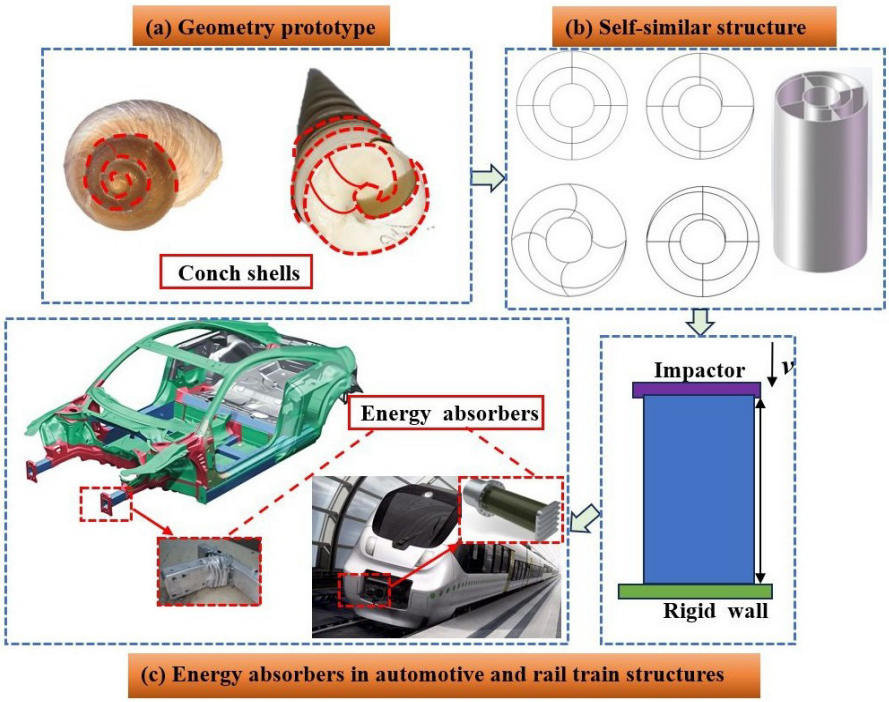

Figure 1 The evolution of bionic structures: (a) biological geometry of conch; (b) cross-sections of biomimetic structure; (c) typical vehicle anti-collision structure and frontal impact absorbers of the vehicle.

2.2.2 Description of the conch shell-inspired bionic tube

In practical engineering applications, a biomimetic tubular structure can be designed as a thin-walled structure composed of an outer tube, an inner tube, a helical plate, and rib plates. Key design variables, such as the pitch (*l*), the number of spirals (*i*), the curvature radius (ρ) of the rib plates, and the number of rib plates (n), are utilized to construct multiple sets of thin-walled tube models inspired by the nautilus shell. These models are employed to optimize their mechanical properties and functional characteristics. As shown in Figures 1(b) and 1(c), the parameter nomenclature and value ranges for the thin-walled tubes with nautilus shell-inspired structures are listed in Table 1.

To facilitate subsequent comparative studies, a naming convention is established for the thin-walled tubes. Taking the naming code BA4-25S1.5-20 as an example, “B” indicates a biomimetic design, “A4-25” represents four arc-shaped rib plates with a curvature radius of 25 mm, and “S1.5-20” denotes a pitch of 20 mm and a spiral number of 1.5. Additionally, “L” signifies linear rib plates, as exemplified by BL6S10. The prefix “C” designates a conventional thin-walled tube design, while “R” represents the radius of the first circle between the inner and outer circumscribed circles.

Table 1 Thin-walled tube parameter naming and value range.

Parameters	explanation of nomenclature	Numerical range
D_{out}	External diameter	70~100mm
D_{in}	Inner diameter	10~40mm
h	Height of thin-walled tube	200mm
ρ	Radius of curvature of circular ribbed plate	15~30mm
n	Rib plate circumferential array number, n is an integer	4~8
t	Thin-walled tube wall thickness	1mm
l	Pitch, radial distance between two neighboring points with a difference of 2π	10-30mm
i	Spiral number, the number of revolutions of the helix around the center axis	1~3

2.3 Fabrication of Thin-Walled Tube Specimens

To thoroughly investigate the energy absorption characteristics of thin-walled tubes with conch shell-inspired structures, this study employed wire-cut electrical discharge machining (EDM) to fabricate AA6061-O aluminum alloy thin-walled tube specimens. This technique, rooted in electrical discharge machining, enables precise processing of metal materials. The specimens were designed as cylindrical tubes with a diameter of 100 mm, a height of 200 mm, and a wall thickness of 1 mm. Considering the adaptability of the manufacturing process, four types of thin-walled tubes with different rib plate structures (each with four rib plates) were selected for this experiment. Two specimens were prepared for each structure, resulting in a total of eight specimens for subsequent axial quasi-static compression tests and drop hammer impact tests (as shown in Figure 2). Table 2 details the structural parameters of the specimens. This design effectively facilitates the comparison of the influence of structural features, such as pitch, rib plate shape, and helical lines, on energy absorption performance. Minor mass variations among specimens of the same type were observed due to machining precision limitations. Note: mm represents the unit of length (millimeter); g represents the unit of mass (gram).



Figure 2 Thin-walled tube samples.

Table 2 Parameter values for processing thin-walled tubes.

Model sample	n	D_{out} (mm)	D_{in} (mm)	l (mm)	R (mm)	i	m (g)	h (mm)	t (mm)
$CL_4R_{1\text{-}35}$	4	100	40	-	35	1	320.8/ 321.3	200	1.0
$BL_4S_{1\text{-}30}$				30	-	1	315.2/ 312.8		
$BA_{4\text{-}20}S_{1\text{-}30}$				30	-	1	323.1/ 334.7		
$BL_4S_{1.5\text{-}20}$				25	-	1.5	386.3/ 392.6		

2.4 Testing Equipment

2.4.1 Quasi-Static Compression Test

Thin-walled structures exhibit significant mechanical characteristics under axial compression conditions: their collapse load demonstrates excellent stability, and their energy absorption capacity is notably superior to that under transverse compression. Studies have shown that the energy absorption efficiency under axial compression is approximately 10 times that under transverse compression [Alghamdi,2001]. To systematically investigate the influence of structural parameters, such as pitch, rib plate shape, and spiral number, on the energy absorption performance of thin-walled structures, this study conducted axial quasi-static compression tests using an ETM 300KN electronic universal testing machine (the tests were performed at the Key Laboratory of Bionic Engineering, Ministry of Education, Jilin University), as shown in Figure 3. During the experiment, a small amount of lubricant was applied between the indenter bottom and the specimen top to minimize friction effects. The test was conducted in displacement control mode, with the platen descent speed set to 5 mm/min. Based on the specimen height of 200 mm, the compression displacement was set to 150 mm, reaching 75% of the specimen height, to ensure the complete recording of the compression deformation process. The testing machine's data acquisition system dynamically recorded key parameters, such as load, displacement, and peak load, to obtain the load-displacement curve. Additionally, the high-speed camera system was employed to record the entire deformation process of the specimen.



Figure 3 Universal Testing Machine.

2.4.2 Impact Resistance Test

To investigate the impact resistance of thin-walled structures under dynamic loading conditions, this study selected bionic thin-walled tubes and conventional thin-walled tubes for drop hammer impact tests. The tests were conducted using a high-energy drop hammer impact testing machine at the Lightweight Vehicle Research Institute of Tsinghua University Suzhou Automotive Research Institute, as shown in Figure 4. The primary technical parameters of the equipment are as follows: maximum impact velocity of 11 m/s, hammer mass range of 36–225 kg, and maximum impact energy of 14,000 J, making it widely applicable for dynamic impact tests on materials, structures, battery modules, and more. Based on the results of quasi-static compression experiments, the minimum impact energy threshold was set to 5,000 J. Applying the law of conservation of energy, the test parameters were determined through theoretical calculations: drop height of 2.67 m, hammer mass of 306 kg, initial velocity of 0 m/s, and impact velocity of 7.23 m/s, ensuring the specimens reached a 70% level of damage. A flat-headed hammer with a base area of 300 mm × 300 mm was used, providing a contact area (90,000 mm^2) significantly larger than the minimum requirement of 7,850 mm^2. The drop hammer impact test employed a 200 kHz sampling rate, utilizing a PCB 356A01 triaxial accelerometer with an 8 kHz cutoff frequency Butterworth filter. All channels were synchronized via an NI PXIe-5171R acquisition card. During the experiment, the hammer was released in free fall via remote control. The transient acceleration signals during impact were acquired using an accelerometer mounted on the drop hammer, and the instantaneous impact load was calculated based on the hammer's mass. Simultaneously, a high-speed camera and dynamic image sequence system were employed to record the deformation process of the specimens, facilitating quantitative analysis of the dynamic deformation patterns of the thin-walled structures.



Figure 4 Drop hammer impact testing machine.

3 RESULTS AND DISCUSSION

3.1 Quasi-Static Compression Performance Comparison

Figure 5 shows the load-displacement curves from quasi-static compression tests of bionic thin-walled tubes and conventional thin-walled tubes. The results indicate that when the compression displacement reaches 140 mm, all specimens enter the densification stage, which represents the actual maximum effective compression displacement. Based on the load-displacement curves, the mechanical performance metrics of each specimen were obtained: the total energy absorption values for CL4R1-35, BL4S1-30, BL4S1.5-20, and BA4-20S1-30 were 4103.14 J, 3971.24 J, 4980.84 J, and 3931.13 J, respectively; their corresponding peak loads were 52.67 kN, 48.34 kN, 56.69 kN, and 46.37 kN. To further evaluate the crashworthiness of the structures, specific energy absorption (SEA), mean crushing force (MCF), crushing force efficiency (CFE), and undulation of load-carrying capacity (ULC) were selected as evaluation metrics, and the comparison results are shown in Figure 6(a).

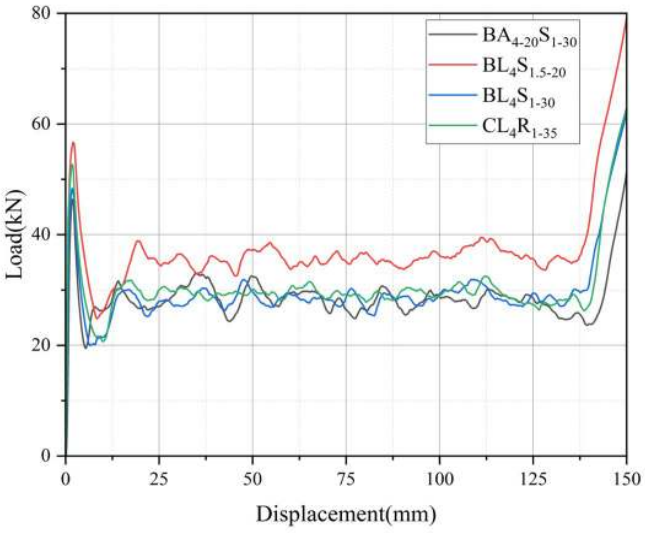

Figure 5 Load-displacement curves of thin-walled tubes.

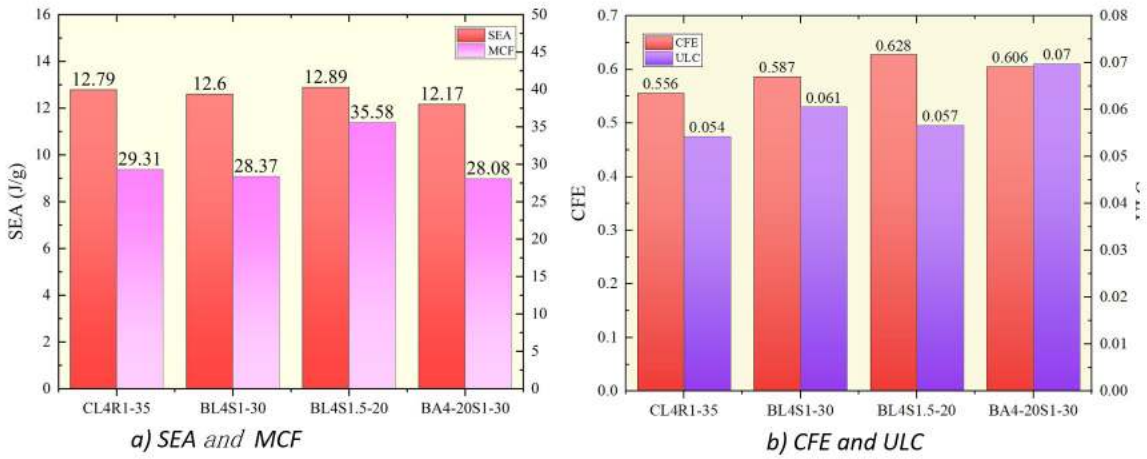

Figure 6 Comparison of Energy Absorption Characteristics of Thin-Walled Tubes.

3.1.1 Influence of Helical Structures on the Performance of Thin-Walled Tubes

Under identical conditions of rib shape and quantity, the deformation characteristics and energy absorption performance of the conventional thin-walled tube CL4R1-35 and the bionic thin-walled tube BL4S1-30 were comparatively analyzed. As illustrated in Figure 7, CL4R1-35 exhibits a progressive deformation mode from bottom to top, while BL4S1-30 follows a deformation path from top to bottom. From an energy dissipation perspective, the top-initiated deformation mode demonstrates higher energy absorption efficiency as its folding wave propagation aligns with the loading direction. In contrast, bottom-initiated propagation tends to induce local stress concentration due to wave superposition effects. According to the conclusions of dynamic compression studies on cylindrical tubes [Du and Song, 2004], the concentrated deformation characteristics at the impact end align with the deformation behavior of BL4S1-30. After the initial wrinkling, BL4S1-30 forms progressive buckling deformation through layer-by-layer superposition. Further analysis of the deformation characteristics reveals that both tubes develop layered wrinkling structures at the junction regions between the ribs and the circumscribed circle. However, the bionic thin-walled tube BL4S1-30 demonstrates higher wrinkling density and shorter folding wavelengths. These structural features collectively confirm that the bionic thin-walled tube possesses enhanced energy dissipation capabilities.

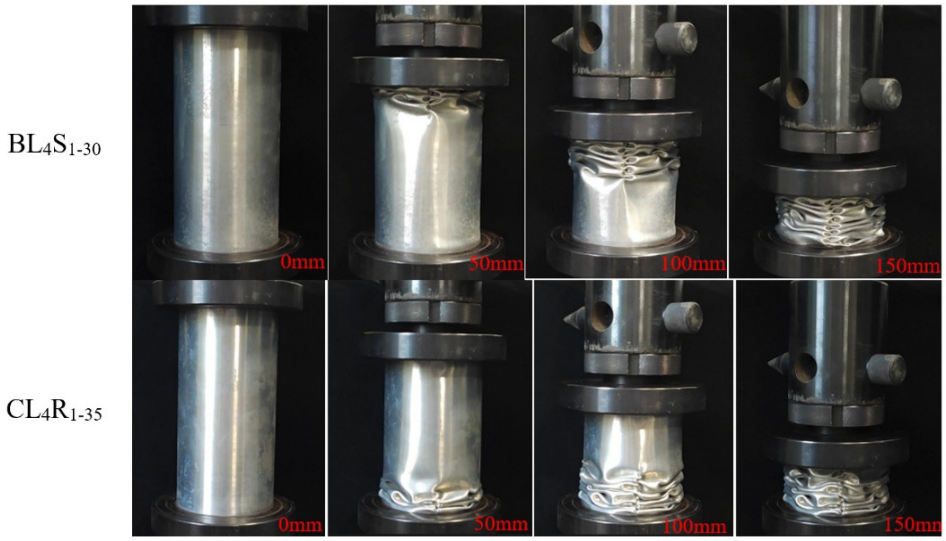

Figure 7 *Deformation process of thin-walled tubes* $BL_4S_{1\text{-}30}$ *and* $CL_4R_{1\text{-}35}$.

The comparative analysis of energy absorption metrics based on Figure 6 reveals that the specific energy absorption (SEA) and mean crushing force (MCF) of BL4S1-30 and CL4R1-35 exhibit minimal differences, with values of 0.19 J/g and 0.94 kN, respectively. However, the peak crushing force (PCF) of the bionic thin-walled tube BL4S1-30 is significantly reduced by 4.33 kN (an 8.96% decrease) compared to the conventional thin-walled tube. Additionally, BL4S1-30 demonstrates notable advantages in crushing force efficiency (CFE) and undulation of load-carrying capacity (ULC), which are improved

by 8.9% and 12.3%, respectively, over the conventional tube. These data fully illustrate that the energy absorption process of the bionic thin-walled tube exhibits higher stability and energy utilization efficiency. A comprehensive analysis of the performance metrics indicates that, under identical structural parameters, the introduction of a bionic helical design enhances the energy absorption characteristics of the thin-walled tube. Specific improvements include a reduction in the initial peak load, enhanced structural stability, and an optimized energy absorption mode. This confirms the effectiveness of the bionic design in improving the crashworthiness of thin-walled tubes.

3.1.2 Influence of Rib Shape on the Performance of Thin-Walled Tubes

Under identical experimental conditions, the deformation processes and energy absorption characteristics of two bionic thin-walled tubes, BL4S1-30 (straight ribs) and BA4-20S1-30 (arc-shaped ribs with a curvature radius ρ=20 mm and pitch l=30 mm), were comparatively analyzed. As shown in Figure 8, both structures exhibit a top-to-bottom layered wrinkling deformation mode. Analysis of the deformation characteristics reveals that BL4S1-30 demonstrates a well-distributed wrinkling pattern, whereas BA4-20S1-30 exhibits longer wrinkling wavelengths, which is detrimental to effective energy absorption. Further observation indicates that the wrinkles are predominantly concentrated at the junction regions between the ribs and the circumscribed tube. Notably, the straight rib design (BL4S1-30) facilitates the formation of shorter-wavelength symmetric wrinkles compared to the arc-shaped rib design (BA4-20S1-30). This structural feature contributes to enhanced energy absorption efficiency.



Figure 8 *Deformation process of thin-walled tubes* BL_4S_{1-30} *and* $BA_{4-20}S_{1-30}$.

The comparative analysis of energy absorption metrics based on Figure 6 reveals differences in energy absorption performance between BL4S1-30 and BA4-20S1-30. Specifically, BA4-20S1-30 exhibits a 3.43% reduction in specific energy absorption (SEA) and a 1.02% decrease in mean crushing force (MCF) compared to BL4S1-30, while its crushing force efficiency (CFE) is improved by 3.19%. However, the undulation of load-carrying capacity (ULC) of BA4-20S1-30 increases by 15.18% relative to BL4S1-30, indicating that while the arc-shaped rib design enhances CFE, it compromises structural stability, leading to an overall decline in energy absorption performance. These findings highlight the critical influence of rib shape on the energy absorption characteristics of thin-walled structures and provide essential insights for structural optimization.

3.1.3 Influence of Pitch and Helical Turns on the Performance of Thin-Walled Tubes

Under identical experimental conditions, this study conducted a comparative analysis of the performance characteristics of two bionic thin-walled tubes, BL4S1-30 and BL4S1.5-20, with distinct structural parameters. Specifically, BL4S1-30 features a pitch of 30 mm and a single helical turn (1 turn), while BL4S1.5-20 has a pitch of 20 mm and 1.5 helical turns. Both samples maintain consistent circle spacing and utilize straight rib designs, aiming to investigate the influence of pitch and helical turns on the deformation process and energy absorption performance. As illustrated in Figure 9, the deformation processes of both structures exhibit ideal predictability. Deformation initiates at the top and develops in a progressive folding mode, forming well-defined and regular wrinkles. These wrinkles are arranged in an orderly and layered manner, demonstrating a typical progressive collapse deformation mechanism.



Figure 9 Deformation process of thin-walled tubes $BL_4S_{1\text{-}30}$ and $BL_4S_{1.5\text{-}20}$.

Figure 6 presents a comparative analysis of energy absorption metrics between thin-walled tubes BL4S1.5-20 and BL4S1-30. The data show that BL4S1.5-20 achieves a 2.30% higher specific energy absorption (SEA) and 25.42% greater mean crushing force (MCF) compared to BL4S1-30. Performance metrics also indicate BL4S1.5-20 exhibits 11.3% lower undulation of load-carrying capacity (ULC) and 5.9% higher crushing force efficiency (CFE). These measured differences suggest that modifications to helical structural parameters - particularly reduced pitch and increased number of helical turns - may influence the energy absorption characteristics of thin-walled structures.

The quasi-static compression tests demonstrate measurable differences in energy absorption characteristics among the four thin-walled tube structures. The bionic design BL4S1.5-20 shows a 21.39% increase in mean crushing force (MCF) and 12.95% improvement in crushing force efficiency (CFE) compared to the conventional tube. The specific energy absorption (SEA) values differ by 0.1 J/g, while the undulation of load-carrying capacity (ULC) varies by 0.003. These results suggest that structural parameter optimization may influence energy absorption performance, though the practical significance of the small SEA and ULC differences requires further investigation.

3.2 Comparative Analysis of Drop Hammer Impact Performance

Under identical impact energy test conditions, this study conducted a comparative analysis of the crushing behavior among the conventional thin-walled tube CL4R1-35 and the three bionic thin-walled tubes: BL4S1-30, BA4-20S1-30, and BL4S1.5-20. The measured actual crushing displacements for the thin-walled tube are as follows: CL4R1-35 (175.19 mm), BL4S1-30 (175.65 mm), BA4-20S1-30 (172.92 mm), and BL4S1.5-20 (167.11 mm). The data presented in Figure 10 represent the raw force measurements obtained from field tests after CFC 180 filtering, where CFC 180 has a cutoff frequency of 300 Hz. Analysis of the load-displacement curves reveals that all specimens enter the densification phase when the crushing displacement reaches 150 mm. Accordingly, the effective crushing displacements are determined as: BL4S1-30 (142 mm), CL4R1-35 (139 mm), BA4-20S1-30 (143 mm), and BL4S1.5-20 (138 mm). As illustrated in Figure 10, the total energy absorption for each specimen, calculated by integrating the load-displacement curves, is as follows: BL4S1-30 (4486.07 J), CL4R1-35 (4328.72 J), BA4-20S1-30 (4822.15 J), and BL4S1.5-20 (5490.25 J).

To systematically assess the impact resistance of the structures, this study selected specific energy absorption (SEA), peak crash force (PCF), mean crash force (MCF), crash force efficiency (CFE), and undulation of load-carrying capacity (ULC) as the key evaluation parameters for the crashworthiness characteristics of thin-walled tubes. Figure 11 presents a comparative analysis of these mechanical performance indicators for the four different thin-walled structures.

3.2.1 Influence of Helical Lines on Thin-Walled Tube Performance

Under constant experimental conditions, while maintaining consistent geometric configurations and quantity parameters of the ribs, this study comparatively analyzed the impact resistance characteristics of the conventional thin-walled structure CL4R1-35 and the bio-inspired optimized structure BL4S1-30. Based on the dynamic crushing process recorded by high-speed photography (Figure 12), the analysis reveals that the conventional thin-walled tube CL4R1-35 exhibited initial deformation at the hammer contact end when the crushing displacement reached 30 mm, subsequently developing into an asymmetric crushing mode at both ends, with an evident non-uniform distribution of folds. In

contrast, the bio-inspired thin-walled tube BL4R1S1-30 displayed a progressive deformation characteristic from top to bottom, with uniform fold distribution.

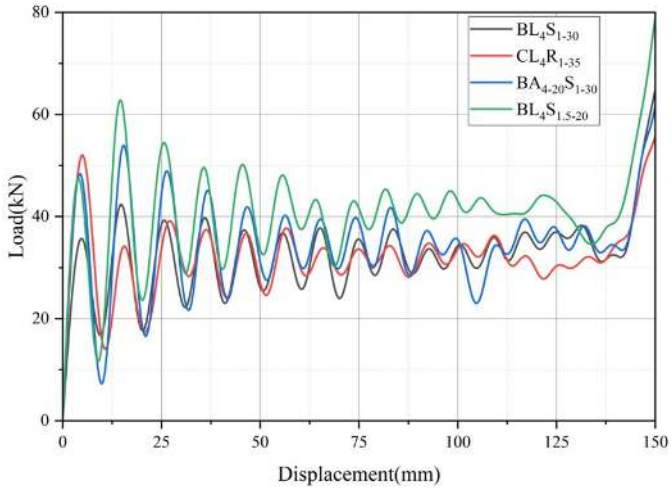

Figure 10 The drop test load-displacement curve.

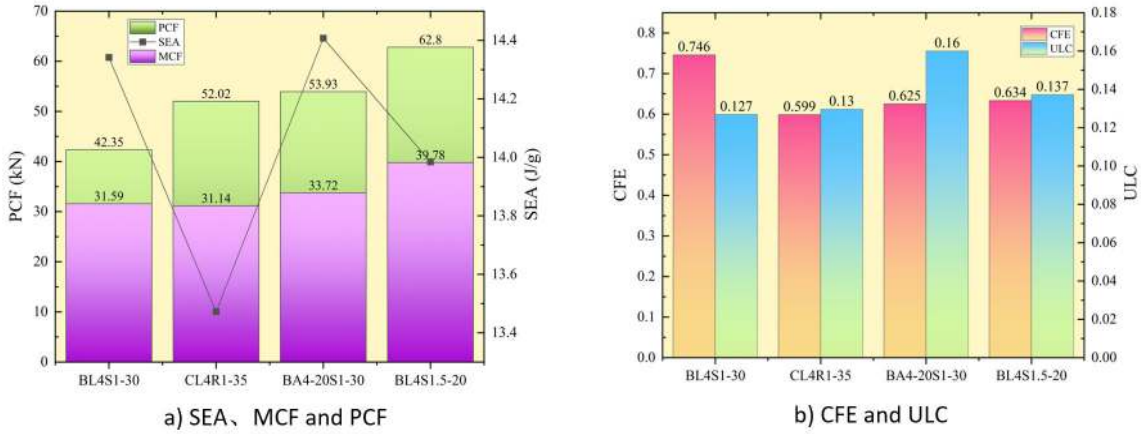

Figure 11 Comparison of Energy Absorption Characteristics of Thin-Walled Tubes.

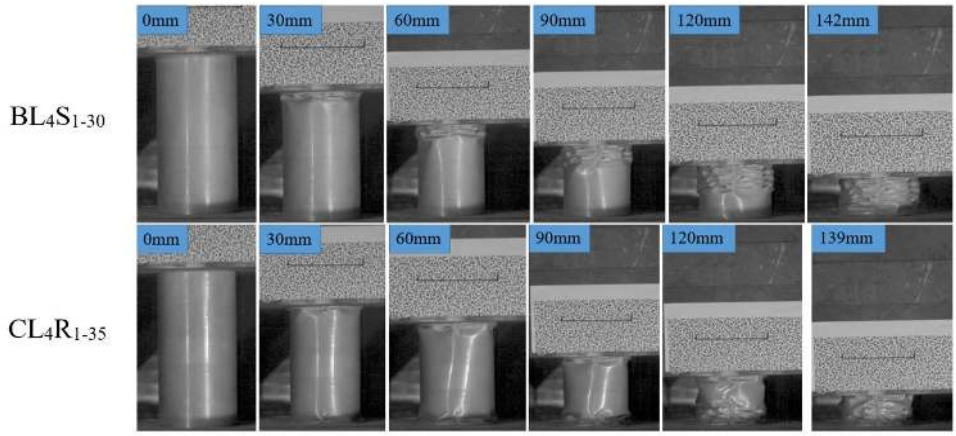

Figure 12 *Deformation process of thin-walled tubes* BL_4S_{1-30} *and* CL_4R_{1-35}.

The comparative analysis of energy absorption characteristics based on Figure 11 reveals that although the bio-inspired thin-walled tube BL4S1-30 and the conventional thin-walled tube CL4R1-35 exhibit similar ultimate crushing displacements, the latter enters the densification stage earlier, resulting in a relatively shorter effective crushing displacement. Under standardized impact conditions, the bio-inspired tube demonstrates measurable performance

differences. BL4S1-30 with a specific energy absorption (SEA) of 14.34 J/g, representing an approximate 6.5% improvement over CL4R1-35 (13.47 J/g). Furthermore, the mean crash force (MCF) and crash force efficiency (CFE) of BL4S1-30 are higher than those of the control group, while its undulation of load-carrying capacity (ULC) is comparatively lower, indicating more stable deformation characteristics and reduced load fluctuations during the impact process. Notably, the PCF of BL4S1-30 measures 42.35 kN, representing a 18.6% reduction compared to CL4R1-35 52.02 kN, which correlates with improved impact structural characteristics. The analysis results demonstrate that under constant structural parameters, the bio-inspired thin-walled tube BL4S1-30 achieves a more stable deformation mechanism under high-speed impact.

The load-displacement curves of thin-walled tubes BL4S1-30 and CL4R1-35 under quasi-static and dynamic loading conditions are compared in Figure 13. The results show that under dynamic loading, the load fluctuation amplitude increases and the total energy absorption (EA) decreases compared to quasi-static conditions. For the bio-inspired thin-walled tube BL4S1-30, the peak crushing force (PCF) decreases under dynamic loading, while the conventional thin-walled tube CL4R1-35 maintains nearly identical PCF values. The results indicate that when other structural parameters of thin-walled tubes remain the same, incorporating bio-inspired spiral lines in the design can effectively improve the impact resistance and energy absorption characteristics of thin-walled tubes, while reducing the initial peak load.

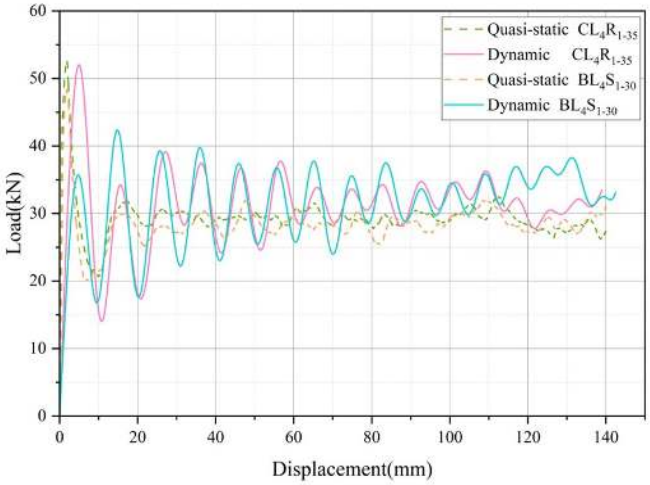

Figure 13 Dynamic and quasi-static load-displacement curves for thin-walled tubes BL_4S_{1-30} and CL_4R_{1-35}.

3.2.2 Influence of Rib Shape on Thin-Walled Tube Performance

Under constant dynamic impact conditions, this study comparatively analyzes the impact resistance performance of two bio-inspired thin-walled tubes (BL4S1-30 and BA4-20S1-30) with different rib configurations. BA4-20S1-30 incorporates arc-shaped ribs with a curvature radius of ρ=20 mm, while BL4S1-30 features straight ribs, with both structures maintaining identical helical parameters (pitch l and number of spirals i). Observations based on the dynamic crushing process illustrated in Figure 14 reveal that both structures exhibit plastic deformation characteristics initiated at the ends under impact loading, with folding patterns characteristic of progressive buckling collapse modes. However, BA4-20S1-30 demonstrates longer fold wavelengths accompanied by localized deformation phenomena. Analysis of the deformation zones indicates that folds primarily form at the joining regions between the ribs and the outer circular tube, suggesting that the geometric shape of the ribs significantly influences the fold formation mechanism and crushing mode under dynamic loading. Specifically, the arc-shaped rib design may lead to a redistribution of stress, thereby affecting the structural deformation characteristics.

The experimental results reveal differences in the mechanical performance between the BL4S1-30 and BA4-20S1-30 thin-walled tubes. BA4-20S1-30 exhibits a smaller ultimate crushing displacement and an earlier onset of densification, with its specific energy absorption (SEA) increasing by only 0.065 J/g compared to BL4S1-30. While its mean crash force (MCF) increases by 2.13 kN, it shows lower crash force efficiency (CFE) and a 26.10% increase in undulation of load-carrying capacity (ULC), indicating instability in its energy absorption process. The overall peak crash force (GPCF) for both specimens occurs at the second peak of the curve, with BA4-20S1-30 showing a 27.34% increase compared to BL4S1-3. This demonstrates that the geometric configuration of the ribs influences load fluctuation characteristics during impact. Further comparison of the response characteristics under dynamic and quasi-static loading (Figure 15) demonstrates that BA4-20S1-30 exhibits similar initial peak crash forces (IPCF) under both conditions. However, its

overall peak crash force under dynamic loading is significantly higher than its quasi-static value, whereas BL4S1-30 shows a decreasing trend. Experimental data indicate that BA4-20S1-30 consistently exhibits higher ULC values under both conditions compared to BL4S1-3. Under equivalent impact energy, BA4-20S1-30 achieves an energy absorption efficiency of 60.23%. In summary, the shape of ribs has relatively small effects on energy absorption per unit mass and displacement. Rib geometry mainly affects load fluctuations and deformation stability.

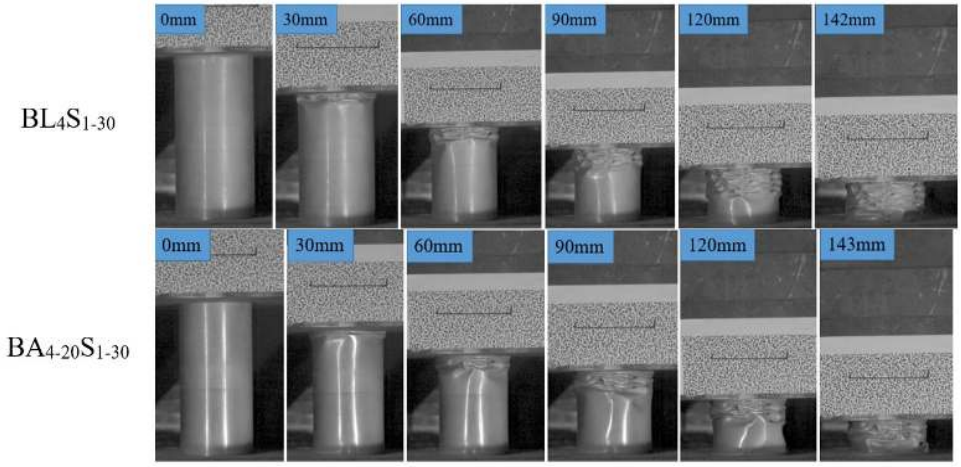

Figure 14 *Thin-walled tube* $BL_4S_{1\text{-}30}$ *and* $BA_{4\text{-}20}S_{1\text{-}30}$ *deformation process*

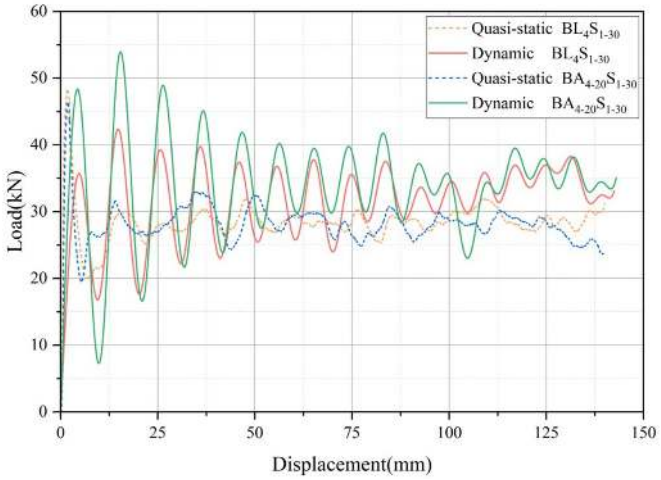

Figure 15 *Dynamic and quasi-static load-displacement curves for thin-walled tubes* $BL_4S_{1\text{-}30}$ and $BA_{4\text{-}20}S_{1\text{-}30}$.

3.2.3 Influence of Pitch and Number of Spirals on the Performance of Thin-Walled Tubes

Under identical working conditions, this study compared the impact resistance performance of the bionic thin-walled tubes BL4S1-30 and BL4S1.5-20. The primary differences in their parameters lie in the spiral characteristics: the pitch (l) is 30 mm for BL4S1-30 and 20 mm for BL4S1.5-20, while the number of spirals (i) is 1 for BL4S1-30 and 1.5 for BL4S1.5-20. However, both tubes share the same rib shape (linear) and the spacing between the inner and outer circles. Through the drop-weight impact tests illustrated in Figure 16, differences in the deformation modes of the two structures were observed. In terms of deformation characteristics, BL4S1.5-20 exhibited progressive folding deformation starting from the bottom, whereas BL4S1-30 began to deform from the top. Despite this, both structures demonstrated typical progressive folding patterns with the following common features: (1) the distribution of folds displayed good symmetry; (2) the layer-by-layer folding process was orderly and regular; and (3) the wavelengths of the folds were similar. Notably, BL4S1.5-20 showed a shorter final crushing displacement, which can be attributed to its higher energy absorption efficiency. To achieve a crushing displacement comparable to other thin-walled structures, a greater impact energy is required for BL4S1.5-20. These results indicate that the pitch (l) and the number of spirals (i) significantly influence the impact resistance performance of thin-walled tubes. Specifically, a smaller pitch (20 mm) combined with a larger number of spirals (1.5 turns) leads to higher energy absorption efficiency but necessitates greater impact energy to achieve a crushing displacement comparable to other structures.

According to the experimental data analysis of energy absorption metrics depicted in Figure 11, the specific energy absorption (SEA) of BL4S1.5-20 decreased by 2.5% compared to BL4S1-30. Meanwhile, its mean crushing force (MCF) and peak crushing force (PCF) increased by 8.19 kN and 20.45 kN, respectively, indicating that BL4S1.5-20 exhibits higher energy absorption capacity per unit crushing displacement but reduced efficiency in energy absorption per unit mass. Compared to BL4S1-30, BL4S1.5-20 demonstrated greater fluctuation in undulation of load-carrying capacity (ULC) and lower crushing force efficiency (CFE), revealing instability in the energy absorption process and significantly enhanced load fluctuations under high-speed impact conditions. The experimental results demonstrate that, with other structural parameters held constant, the pitch and number of spirals in the spiral structure significantly influence the impact resistance performance of thin-walled structures. Specifically, a smaller pitch combined with a higher number of spiral turns does not notably enhance the crashworthiness of the structure; instead, it leads to an increase in peak load values and exacerbates load fluctuations.

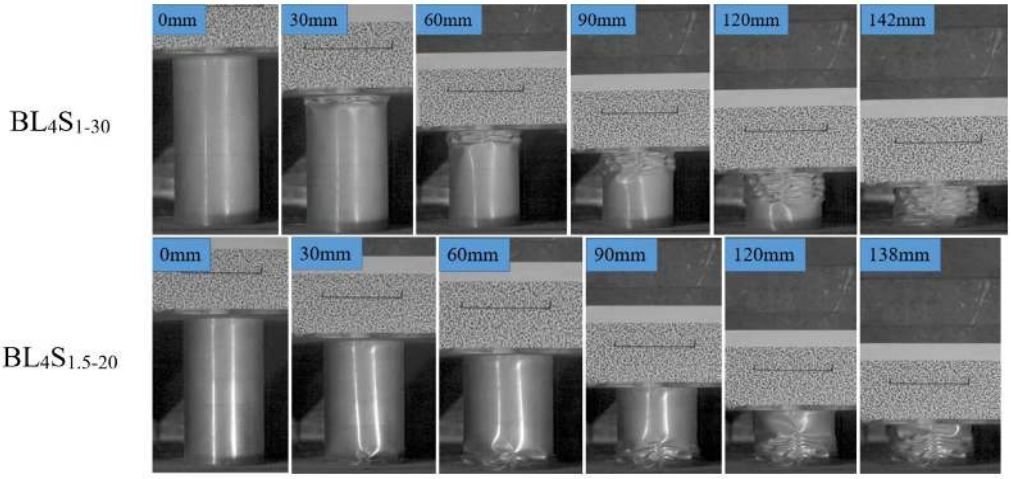

Figure 16 Deformation process of thin-walled tubes $BL_4S_{1\text{-}30}$ and $BL_4S_{1.5\text{-}20}$.

The load-displacement curves in Figure 17 demonstrate distinct mechanical responses of BL4S1.5-20 and BL4S1-30 under different loading conditions, with all specimens exhibiting multi-stage failure characteristics under dynamic loading. For BL4S1.5-20, the initial peak load under dynamic loading decreases compared to static loading, while the secondary peak load shows an increase. The overall peak load occurs at the second wave crest and exceeds the quasi-static peak load. In contrast, BL4S1-30 generally exhibits lower peak loads than BL4S1.5-20 under dynamic conditions, with its maximum load appearing during the second wave crest phase. Consequently, BL4S1-30 demonstrates superior energy absorption performance compared to BL4S1.5-20 under both quasi-static and dynamic impact conditions.

The comprehensive evaluation results derived from drop-weight impact tests indicate that under dynamic loading, all four thin-walled structures exhibited multi-peak characteristics in their load-displacement curves, with the peak load of the bionic thin-walled tubes consistently appearing at the second peak. This phenomenon indicates that the structure can withstand impact load and undergo plastic deformation during the initial stage, while the maximum load occurs after the initial peak, validating the nonlinear failure characteristics during the drop-weight impact process. Among the four thin-walled tube structures, the bionic thin-walled tubes BL4S1-30 and BA4-20S1-30 exhibit the most energy absorption performance. Specifically, their specific energy absorption (SEA) values increased by 6.4% and 6.9%, respectively, compared to ordinary thin-walled tubes, while the mean collision force (MCF) also demonstrated growth. Notably, the bionic thin-walled tube BL4S1-30 not only exhibited reduction in peak load but also achieved a 24.61% improvement in crushing force efficiency (CFE) compared to ordinary thin-walled tubes. Additionally, the fluctuation in undulation of load-carrying capacity (ULC) for this structure was significantly reduced, indicating more stable deformation behavior during the impact process. This experiment reveals the dynamic mechanical response patterns of thin-walled structures, providing essential experimental evidence and theoretical guidance for optimizing spiral structure parameters and enhancing structural impact resistance performance.

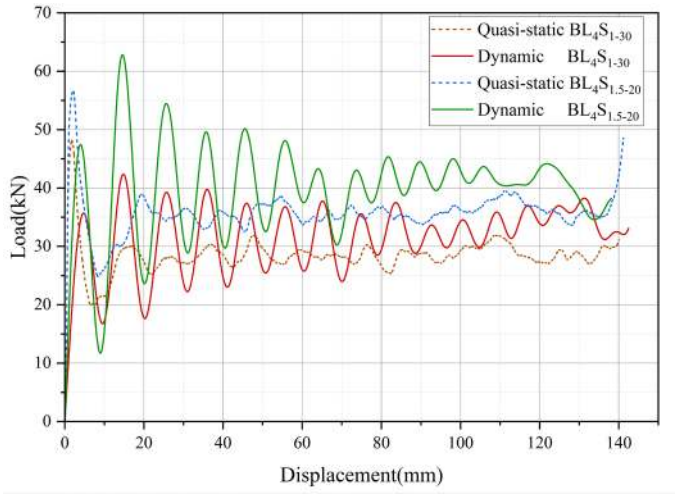

Figure 17 Schematic representation of inverse crack propagation analysis.

4 CONCLUSION

Based on the biological characteristics of conch shells, this study developed bio-inspired thin-walled structures incorporating spiral lines, circumscribed circular (conical) tubes, inscribed circular (conical) tubes, and rib plates. A total of eight specimens were prepared, divided into two groups (two ordinary thin-walled tubes and six bio-inspired thin-walled tubes). Quasi-static compression and drop-weight impact tests were performed to systematically investigate the influence mechanisms of spiral line parameters, rib plate configurations, and pitch on the deformation modes and energy absorption characteristics of the structures.

The quasi-static test results indicate that the bio-inspired thin-walled tube BL4S1.5-20 exhibits the most superior performance, demonstrating a progressive buckling deformation mode with excellent fold symmetry. Compared to conventional structures, the mean crushing force (MCF) of this specimen increased by 21.39%, and the crushing force efficiency (CFE) improved by 12.95%. Dynamic load tests revealed that the load-displacement curves of all specimens exhibited multi-peak characteristics, with the maximum load occurring after the initial peak. Among them, the bio-inspired thin-walled tube BL4S1-30 displayed the most outstanding performance metrics: a significant reduction in peak load, simultaneous improvement in specific energy absorption (SEA) and MCF, and a CFE increase of 24.61%. Additionally, the fluctuation of the undulation of load-carrying capacity (ULC) was significantly reduced, indicating the most stable deformation process.

A comprehensive analysis reveals that the bio-inspired design elements significantly influence structural performance: (1) The introduction of spiral lines markedly enhances structural performance; (2) The configuration of rib plates is a critical factor affecting energy absorption characteristics, with arc-shaped rib plates reducing performance; (3) The pitch and number of spirals exhibit notable performance differences under quasi-static and dynamic conditions, with smaller pitches yielding better overall performance under quasi-static loading. The experimental results confirm that the optimized design based on mollusk shell biomimicry effectively improves the energy absorption efficiency and mechanical stability of thin-walled structures, providing a theoretical foundation for engineering impact protection design. Future research can explore its application in diverse loading scenarios.

Acknowledgments

This research was funded by the Technological Planning Projects of First Division Alar City, Xinjiang Construction Corps(2024GX04).

Author's Contributions: Conceptualization,ZH.Guo.and N.Han.; Writing-original draft, ZH.Guo. and N.Han.; Methodology, M.Zou.; Investigation, N.Han.; Formal analysis, ZH.Guo.; Writing-review & editing, ZH.Guo.and N.Han.; Funding acquisition, ZH.Guo; Project administration, J.Liu.; Resources, ZH.Guo.and N.Han; Validation and Software, YS.Liu.

Data availability: Research data is available in the body of the article.

Editor: Marcílio Alves

References

Wu, J.C., Zhang, Y., Zhang, F., Hou, Y.B., Yan, X.L.(2021). A bionic tree-liked fractal structure as energy absorber under axial loading. Engineering Structures, 245.

Li, R.X., Zhao, Z.W., Bao, H.H., Pan, Y.J., Wang, G.X., Liu, B.H., Liao, T.J., Li, J.(2024). Bio-inspired honeycomb structures to improve the crashworthiness of a battery-pack system. Engineering Failure Analysis, 158.

Zhang, Y., Wang, J., Wang, C.H., Zeng, Y., Chen, T.T.(2018a). Crashworthiness of bionic fractal hierarchical structures. Materials & Design, 158: 147-159.

Tang. Z., Liu. S., Zhang. Z.(2013). Analysis of energy absorption characteristics of cylindrical multi-cell columns. Thin-Walled Structures, 62: 75-84.

Chen. Y., Deng. X., Huang. H., et al.(2023). Crashworthiness of bionic tree-shaped hexagonal hierarchical gradient structures under oblique crushing conditions. Mechanics of Advanced Materials and Structures, 1-21.

Wang.W., Ye.W., Huang. K., et al.(2023). Impact-resistance mechanism of gradient ceramic/high entropy alloy composite structure. Mechanics of Advanced Materials and Structures, 1-13.

Sun. G., Chen. D., Zhu. G., et al.(2022). Lightweight hybrid materials and structures for energy absorption: A state-of-the-art review and outlook. Thin-Walled Structures, 172: 108760.

Albak. E, I.(2021). Crashworthiness design for multi-cell circumferentially corrugated thin-walled tubes with sub-sections under multiple loading conditions. Thin-Walled Structures, 164: 107886.

Tran. T. .N., Baroutaji. A.(2018). Crashworthiness optimal design of multi-cell triangular tubes under axial and oblique impact loading. Engineering Failure Analysis, 93: 241-256.

Abdullahi. H, S., Gao. S.(2020). A novel multi-cell square tubal structure based on Voronoi tessellation for enhanced crashworthiness. Thin-Walled Structures, 150: 106690.

Shi long Wang,Yang Liu, Haiying Bao, Zhilai Huang .(2025).Energy absorption and indentation resistance of re-entrant arched honeycomb reinforced by circular ribs. Latin American Journal of Solids and Structures,22.

Zhou, J.F., Liu, S.F., Guo, Z.Q., Xu, S.C., Song, J.F., Zou.(2022). M. Study on the energy absorption performance of bionic tube inspired by yak horn. Mechanics of Advanced Materials and Structures, 29: 7246-7258.

Jiang. B., Tan. W., Bu. X., et al.(2019). Numerical, theoretical, and experimental studies on the energy absorption of the thin-walled structures with bio-inspired constituent element. International Journal of Mechanical Sciences, 164: 105173.

Song. J., Xu. S., Zhou. J., et al.(2021). Experiment and numerical simulation study on the bionic tubes with gradient thickness under oblique loading. Thin-Walled Structures, 163: 107624.

San Ha, N., Pham .T, M., Hao .H., et al. (2021). Energy absorption characteristics of bio-inspired hierarchical multi-cell square tubes under axial crushing. International Journal of Mechanical Sciences, 201: 106464.

Yin. H., Xiao. Y., Wen. G., et al.(2015). Crushing analysis and multi-objective optimization design for bionic thin-walled structure. Materials & Design, 87: 825-834.

Zhang. L., Bai. Z., Bai. F.(2018b). Crashworthiness design for bio-inspired multi-cell tubes with quadrilateral, hexagonal and octagonal sections. Thin-Walled Structures, 122: 42-51.

Song. J.F., Li. G.Y., Liu. Y.S., Zou. M.(2024). Quasi-Static and Dynamic Mechanical Properties of Reed Straw. Latin American Journal of Solids and Structures, 21.

Gao. Z., Zhang. H., Zhao. J., et al.(2023). The axial crushing performance of bio-inspired hierarchical multi-cell hexagonal tubes. International Journal of Mechanical Sciences, 239: 107880.

Ballarini. R., Heuer. A, H.(2007). Secrets in the shell: the body armor of the queen conch is much tougher than comparable synthetic materials. What secrets does it hold?. American Scientist, 95(5): 422-429.

Liu.Y.S., Zou. M., Qi. Y.C., Chen. L.N., Wang. Z.Y., Song. J.F., He, L.B.(2024). Bionic design of thin-walled bilinear tubes with excellent crashworthiness inspired by glass sponge structures. Bioinspiration & Biomimetics, 19.

Wen. M., Li. Z.X., Xie . S.C. (2020). Crashworthiness analysis of thin-walled bio-inspired multi-cell corrugated tubes under quasi-static axial loading. Engineering Structures, 204:110069.

Ghazlan. A., Ngo. T., Le. T.V., Nguyen. T., Remennikov. A.(2020). Blast performance of a bio-mimetic panel based on the structure of nacre - A numerical study. Composite Structures, 234.

Alghamdi. A, A, A.(2001). Collapsible impact energy absorbers: an overview. Thin-walled structures, 39(2): 189-213.

Du Xingwen, Song Hongwei.(2004). Impact Dynamics and Crashworthiness Design of Cylindrical Shells. Science Press.